n-p (Hg,Cd)Te PHOTODIODES FOR 8-14 MICROMETER HETERODYNE APPLICATIONS

J.F. Shanley and C.T. Flanagan

Honeywell Electro-Optics Center
2 Forbes Road
Lexington, Massachusetts 02173

ABSTRACT

This paper presents experimental results describing the dc and CO_2 laser heterodyne characteristics of a three element n^+-p $Hg_{0.8}Cd_{0.2}Te$ photodiode array and single element and four element n^+-n^--p $Hg_{0.8}Cd_{0.2}Te$ photodiode arrays. The measured data shows that the n^+-p configuration is capable of achieving bandwidths of 475 to 725 MHz and noise equivalent powers of 3.2×10^{-20}W/Hz at 77 K and 1.0×10^{-19}W/Hz at 145 K. The n^+-n^--p photodiodes exhibited wide bandwidths ($\sim$2.0 GHz) and fairly good effective heterodyne quantum efficiencies ($\sim$13-30% at 2.0 GHz). Noise equivalent powers ranging from 1.44×10^{-19}W/Hz to 6.23×10^{-20}W/Hz were measured at 2.0 GHz.

INTRODUCTION

Infrared heterodyne detection as a means of detecting weak signals is useful in many systems applications, such as remote sensing, communications, optical radar range finders, battlefield surveillance, velocity and turbulence measurements and infrared astronomy. Infrared heterodyne receivers which utilize (Hg,Cd)Te photodiodes in a 10.6μm CO_2 laser heterodyne application have been developed for use in these systems. There are two (Hg,Cd)Te photodiode structures which have been designed to meet the needs of various heterodyne applications: the n^+-p photodiode and the n^+-n^--p photodiode.[1-5]

The n^+-p (Hg,Cd)Te photodiode structure was initially designed for use in direct detection systems, and hence, the device detectivity has been optimized.[3-5] There are a number of CO_2 laser heterodyne system applications which require moderate bandwidths ($\sim$500 MHz) and elevated temperature operation ($T \gtrsim 120$ K). The n^+-p photodiode structure is optimum for elevated temperature operation since it is capable of attaining fairly low saturation currents.

It is very difficult to operate n^+-n^--p (Hg,Cd)Te photodiodes at temperatures greater than 110 K due to the low carrier concentration (near intrinsic) contained in the n^--layer. However, the advent of techniques for ultra-wideband modulation of CO_2 laser transmitter signals and the requirement to handle large Doppler frequency offsets has created the need for extending the IF bandwidth performance of infrared receivers to at least 2.0 GHz. The n^+-n^--p (Hg,Cd)Te photodiodes are ideally suited for such applications since they are capable of attaining large IF bandwidths.

This paper presents results pertaining to the two diode structures. The n^+-p photodiode attained heterodyne signal frequency response of 475 - 675 MHz at a temperature of 145 K. Also, the n^+-n^--p photodiode demonstrated bandwidths of 2000 MHz when operated in a heterodyne mode at a temperature of 77 K.

HETERODYNE FIGURE OF MERIT

The noise equivalent power (NEP) offers a very convenient figure of merit for evaluating the heterodyne performance of a (Hg,Cd)Te photodiode. The NEP is defined as the incident signal power that must be detected in order to give a signal-to-noise ratio (SNR) of 1.0 in a bandwidth of 1.0 Hz. The NEP per unit bandwidth for an n-p (Hg,Cd)Te photodiode is given by the following expression:

$$\frac{NEP}{B} = \frac{h\nu}{\eta q}\left\{1 + \frac{I_{SAT}}{I_{LO}} + \frac{2k(Tm + T_{IF})}{qI_{LO}}\left(G_D(1+G_DR_S) + \omega^2C^2R_S\right)\right\} \quad (1)$$

where I_{LO} is the laser local oscillator induced current which is related to the incident laser power through the expression:

$$I_{LO} = \frac{h\nu}{\eta q} P_{LO}. \quad (2)$$

where h is Planck's constant, ν is frequency, q is the electron charge, and η is the dc quantum efficiency.

The last two terms in equation (1) establish the criteria for determining the trade-off between the fractional degradation in NEP as a function of the local oscillator power, using the following quantities as parameters:

- The device equivalent circuit parameters (G_D the shunt conductance, R_S the series resistance, and C_D the junction capacitance),
- The photodiode saturation current (I_{SAT}),
- The physical temperature of the photodiode (T_M),
- The device quantum efficiency (η),
- The IF preamplifier characteristics (T_{IF} the equivalent preamplifier noise temperature).

It is instructive to recast equation (1) by defining a minimum detectable signal power $P_{min} = h\nu/\eta q$, an available thermal noise power,

$$P_{th} = 4k(T_m + T_{IF})B$$

and an available shot noise power,

$$P_{sh} = 2qI_{LO}B/\left(G_D\ (1 + G_D R_S) + \omega^2 C_D{}^2 R_S\right)$$

The NEP can then be written as:

$$\frac{NEP}{B} = P_{min}\left(1 + \frac{I_{SAT}}{I_{LO}} + \frac{P_{th}}{P_{sh}}\right) \qquad (3)$$

In order for the NEP to approach the theoretical limit (P_{min}) the photodiode must be operated under the following conditions:

1. $I_{LO} \gg I_{SAT}$
2. $P_{sh} \gg P_{th}$

For the best heterodyne detection sensitivity, the local oscillator induced current (I_{LO}) is fixed so that the shot noise dominates the thermal noise and the photo-induced current dominates the saturation current so that:

$$\frac{NEP}{B} \approx P_{min} = \frac{h\nu}{\eta q} \qquad (4)$$

Under these conditions the device sensitivity is only limited by the dc quantum efficiency. In reality it is very difficult to adjust the incident local oscillator so that it completely dominates the shot noise and the saturation current. Therefore, the observed NEP is

$$\frac{NEP}{B} = \frac{h\nu}{q\eta_{EH}}$$

where the effective heterodyne quantum efficiency η_{EH} includes the effects contributed by the bracketed term in equation (1). The effective heterodyne

quantum efficiency is, thus, a figure-of-merit which describes quantitatively how closely a given infrared heterodyne receiver (i.e., the (Hg,Cd)Te photodiode and amplifier combination) approaches the maximum theoretical efficiency, i.e., η_{EH} = 100% which corresponds to the quantum noise limited NEP of 1.87 X 10^{-20} W/Hz at a wavelength of 10.6 micrometers.

The (Hg,Cd)Te photodiode device parameters (I_{SAT},G_D,R_S, and C_D)are also very important quantities which must be considered in order to optimize the effective heterodyne quantum efficiency. The ideal (Hg,Cd)Te heterodyne photodiode is one in which the thermally generated detector noise is minimized. This means that the saturation current must be limited to very small values by choosing the (Hg,Cd)Te material with the longest possible minority carrier lifetime and the detector configuration with the smallest volume for thermal generation of electron-hole pairs. Thus, if the saturation current is minimized then moderate levels ($\sim$500 microwatts) of local oscillator power are required to overcome the effects of the thermally generated detector noise (I_{SAT}).

Finally, it is noted that the laser induced shot noise power is dependent upon the photodiode shunt conductance, series resistance, and junction capacitance. The maximum shot noise power is obtained when the device possesses a low series resistance ($\backsim$ 5 to 10 ohms), a low capacitance ($\backsim$ 1.0 to 2.0 pF) and a low shunt conductance ($\backsim$ 1.0 X 10^{-3} to 2 X 10^{-4} mhos). Therefore, in designing the best n-p (Hg,Cd)Te photodiode structure it is necessary to reduce the thermal noise contribution to as low a value as is possible and to minimize the G_D, R_S, and C_D parameters.

THE n^+-p $Hg_{0.8}Cd_{0.2}Te$ PHOTODIODE

The n^+-p photodiode structure possesses low saturation currents because the doping levels in the n and p regions are chosen such that the width of the depletion region is reduced. This, in effect, minimizes the generation-recombination current contributed by the depletion layer. The thermal diffusion current from the n-region is minimized by fabricating a fairly thin n^+-layer

(0.3 to 0.7 micrometers). Therefore, the p-region is the primary source of the saturation current. Reducing the volume of the p-region will also help minimize the thermal diffusion current from the p-side. The bandwidth of the n^+-p photodiode is determined by the lifetime of the minority carriers (electrons) diffusing to the junction from the p-region. This implies that the bandwidth of the n^+-p device will be smaller than the n^+-n^--p device since the bandwidth of the n^+-n^--p device is RC limited and the primary collection mechanism is due to the electric field in the depletion region. However, in order to achieve (Hg,Cd)Te photodiodes that are capable of high sensitivity heterodyne detection at elevated temperatures, one must pay the penalty of loss in bandwidth.

Planar processing techniques were used to fabricate the n^+-junctions on a substrate of copper doped p-type ($N_A \backsim 2.0 \times 10^{16} cm^{-3}$) $Hg_{0.8}Cd_{0.2}Te$. The high carrier n^+ layer ($N_D \backsim 1.0 \times 10^{-18} cm^{-3}$) was achieved by the ion implantation of boron, a slowly diffusing donor species, into the p-type substrate. A double boron ion implantation was employed to achieve n^+-junction depths of approximately 0.3 to 0.7 micrometers. The ions were implanted into photolithographically defined areas and the wafers were then subjected to post-implant thermal anneals. The anneals, which reduce implant induced damage that will mask the electrical activity of the impurity species,[4,5] were performed in a reducing atmosphere of forming gas at temperatures ranging from 125 to 175°C with durations of one to three hours.

Front and backside contacts were made subsequent to the post-implant anneals. A thin gold layer was used for the backside contact. Upon completion of the fabrication procedure, the (Hg,Cd)Te wafer was then diced into chips which were then individually affixed to a high frequency mounting structure.

The characterization of the n^+-p photodiode is made through the use of dc characteristics (I-V characteristics, spectral response, and capacitance-voltage measurements) and shot noise and blackbody heterodyne radiometry measurements. The data obtained from these measurements is presented in Table 1.

The current-voltage (I-V) characteristics of the n^+-p $Hg_{0.8}Cd_{0.2}Te$ photodiodes were measured at 77 K and 145 K. The devices exhibited forward resistances of approximately 20 to 40 ohms at both temperatures, and the zero bias resistance was found to vary from 75 to 7000 ohms at 77 K, while at 145 K the zero bias resistance ranged from 30 to 250 ohms. The breakdown voltage, defined to be that voltage at which 1.0 mA of excess reverse current flows in the junction, varied from approximately 0.20 to 0.75 volts at 77 K and from 0.06 to 1.30 volts at 145 K. Figure 1 shows the current-voltage characteristic of element one of the three element array. Spectral response measurements revealed that the photodiodes possessed cutoff wavelengths of approximately 10.31 to 14.1 micrometers and 8.89 to 11.4 micrometers at 77 K and 145 K, respectively.

Blackbody measurements were performed at a frequency of 1.0 kHz to measure the dC quantum efficiencies of the devices. The result of these measurements are shown in Table 1. The devices are seen to exhibit dC quantum efficiencies ranging from 73% to 78%.

Capacitance-voltage measurements were performed on the three elements of the array; the results of the measurements on element one are shown in Figure 2, where a graph of $1/C^2$ versus the reverse bias voltage at 77 K is presented. The straight line plot reveals that the n^+-p junction is abrupt (i.e. $N_D >> N_A$). The net acceptor concentrations in the p-regions of the array were determined from the line slopes to vary from 1.0×10^{16} to 3.1×10^{16} cm^{-3}. This result is consistent with the initial copper concentration ($N_A \sim 2.0 \times 10^{16}$ cm^{-3}) that was introduced during the growth of the p-type $Hg_{0.8}Cd_{0.2}Te$. In addition, Hall measurements performed at 77 K yielded acceptor concentrations of approximately 1.5×10^{16} to 3.4×10^{16} cm^{-3}.

Shot noise and blackbody heterodyne radiometry techniques were used to measure the n^+-p photodiode's frequency response and noise equivalent power (NEP).[1,2,6,7] The measurements were made with a low noise wide bandwidth preamplifier which possessed a net gain of approximately 35 dB, a noise figure of 2.5 dB, and a bandwidth of 5 to 1000 MHz. The shot-noise frequency response was measured by illuminating the photodiode's active area with sufficient chopped CO_2 laser power to overcome the thermal noise. The shot noise spectrum

was determined by slowly scanning a spectrum analyzer over the induced shot noise and synchronously detecting the chopped signal by connecting a lock-in amplifier to the vertical output of the spectrum analyzer.

The measured shot noise frequency response of the n^+-p photodiode array ranged from 581 to 820 MHz for incident CO_2 laser power levels of 175 to 300 microwatts at 77 K and 145 K. The response did not vary as a function of device temperature.

The heterodyne frequency response and sensitivity (represented by either the noise equivalent power, NEP, or the effective heterodyne quantum efficiency, η_{EH}) were measured using the experimental configuration illustrated in Figure 3. A blackbody source (T = 1000 K) beats against the CO_2 laser local oscillator source. The local oscillator power is adjusted so that the shot noise dominates the thermal noise in the receiver. By measuring the signal-to-noise ratio (SNR), the effective heterodyne quantum efficiency can be calculated from the following expression:

$$SNR = 2\eta_{EH}(B\tau)^{\frac{1}{2}} \chi \left[\frac{\varepsilon_{BB}}{\exp(h\nu/kT_{BB}) - 1} - \frac{\varepsilon_r}{\exp(h\nu/kT_r) - 1} \right] \qquad (5)$$

where τ is the post detection integration time, B is the IF bandwidth, χ is the optics transmission factor, T_{BB} and T_r are the blackbody and reference temperatures and ε_{BB} and ε_r are the emissivities of the blackbody and reference.

Figure 4 presents the heterodyne frequency response for element one measured at 145 K. It is seen to be flat to approximately 600 MHz. The right side of Table 1 presents a summary of the heterodyne properties of the three element n^+-p photodiode array. It also lists the operating points (i.e., reverse bias voltage, capacitance and dark current at the bias voltage, and incident CO_2 laser power) at which the heterodyne measurements were made. The data clearly indicates that it is possible to operate the n^+-p photodiode in the heterodyne mode and to obtain moderate bandwidth (475 - 725 MHz) and fairly good sensitivities, $\eta_{EH} \sim 58\%$ and $\eta_{EH} \sim 19\%$, at 77 K and 145 K, respectively.

THE n^+n^--p $(Hg_{0.8}Cd_{0.2})Te$ PHOTODIODE

The n-i-p photodiode is the optimum (Hg,Cd)Te device structure for use as a high speed, i.e., wide bandwidth, CO_2 laser heterodyne detector of infrared radiation.[8,9] The device consists of a slab of nearly intrinsic "i" semiconductor, bounded on one side by a relatively thin layer of very heavily doped n-type material and on the other side by a relatively thick layer of heavily doped p-type semiconductor material. Ohmic contacts to the heavily doped regions serve as a means of applying sufficient dc reverse bias voltage to the structure so that the depletion layer of the junction spreads out to occupy the entire intrinsic or lightly doped n-volume. This volume then becomes a region of high and nearly constant electric field, a region which is swept free of electron-hole pairs, and one which constitutes the active volume of the device.[10,11]

Absorption of infrared radiation in the semiconductor produces electron-hole pairs that are either collected by the drift (electric field) or diffusion mechanism. For high speed devices, the drift mechanism must dominate since the diffusion mechanism only serves to limit the heterodyne device's high frequency sensitivity. For maximum collection efficiency, the intrinsic region must be tailored to be $2/\alpha$ thick, where α is the absorption coefficient of the incident infrared radiation. Thus, diffusion of carriers from the p-side of the junction is minimized by proper placement of the i region below the surface.

In practice, it is very difficult to achieve the idealized intrinsic layer in most semiconductors, i.e., silicon, gallium arsenide, mercury cadmium telluride, etc. Therefore, the "i" region is approximated by either a lightly doped n-layer or a lightly doped p-layer.[8] It is because of the low doping in the i region that most of the potential drop appears across this region. The n^+-n^--p photodiode is the best (Hg,Cd)Te device structure for wide bandwidth CO2 laser heterodyne applications since this configuration is analogous to the n-i-p photodiode.

Planar processing techniques were used to fabricate the lightly doped n^- layers (active area is 1.8×10^{-4} cm^2) on a substrate of p-type ($N_A \sim 1.0 \times 10^{17}$ cm^{-3}) $Hg_{0.8}Cd_{0.2}Te$.[1,2] The substrates are initially doped with a net donor concentration of approximately 1.0×10^{14} cm^{-3}. A mercury diffusion process which compensates the non-stoichiometric defects, presumably mercury vacancies, in the p-type substrate is employed to convert a surface layer of the p-type material to n-type material. Annealing in a mercury atmosphere allows mercury to diffuse into the p-type substrate and this results in the annihilation of the mercury vacancies, thereby allowing the residual donor impurities already present in the substrate to predominate. A shallow n^+-layer ($N_D \sim 5 \times 10^{17}$ to 1.0×10^{18} cm^{-3}) was applied to the surface of n-layer in order to reduce the device's series resistance.

I-V characteristics measured on the n^+-n^--p photodiodes revealed forward resistances of approximately 10 to 35 ohms and zero bias resistances of 180 to 5000 ohms. The breakdown voltage ranged from 630 to 2250 mV for devices possessing cutoff wavelengths of 10.88 to 12.5 micrometers.

C-V measurements were performed on the n^+-n^--p devices and plots of $1/C^2$ versus the reverse bias voltage have resulted in a straight-line behavior. This indicates that the mercury diffusion process creates a one-sided abrupt junction ($N_A >> N_D$). A least square fit applied to the $1/C^2$ data yielded a net donor concentration of approximately 1.1×10^{14} to 1.0×10^{15} cm^{-3} in the n^- layer. The donor concentrations measured by the C-V technique are consistent with the initial donor concentrations that were introduced during the growth of the p-type $(Hg_{0.8}Cd_{0.2})Te$.

Blackbody measurements performed at a frequency of 1 kHz resulted in dC quantum efficiencies ranging from 34% to 65%. The n^+-n^--p photodiodes did not possess anti-reflection coatings on their active areas.

The shot noise and blackbody heterodyne radiometry techniques already discussed were used to characterize the n^+-n^--p photodiode. The results of the shot-noise measurements indicated that many of the photodiodes tested had frequency responses that were flat to 2.0 GHz; no sign of the RC roll-off was

present at this frequency. However, the frequency response was observed to be a function of the applied reverse bias voltage. Increasing the reverse bias voltage increases the depletion width and, hence, reduces the device capacitance. Since the photodiode shot-noise frequency response is RC limited, reducing the capacitance results in increasing the device frequency response.

The shot-noise frequency response of an n^+-n^--p (Hg,Cd)Te photodiode, with a bandwidth greater than 2.0 GHz, is presented in Figure 5. The observed shot-noise signal level presented in Figure 5 changes as the reverse bias voltage is varied since the device impedance is a function of the reverse bias voltage. Network analyzer measurements presented in Figure 6 show that the voltage standing wave ratio changes as a function of the reverse bias voltage. The data presented in Figure 6 was measured using a computer controlled Hewlett-Packard 8542 network analyzer and clearly shows that the device impedance changes as a function of the applied reverse bias voltage. Similar measurements have also demonstrated that the device impedance is also dependent on the incident CO_2 laser power.[6]

Blackbody heterodyne measurements were made on the n^+-n^--p photodiodes. Effective heterodyne quantum efficiencies were measured in the 100 to 2000 MHz frequency region and ranged from 13 to 30%. These values correspond to noise equivalent powers of 1.44×10^{-19} W/Hz to 6.23×10^{-20} W/Hz, respectively. Table 2 presents a summary of the heterodyne characteristics of single element n^+-n^--p photodiodes while Table 3 presents heterodyne data on a 2 x 2 element array. All of the data presented in this paper was measured on devices possessing a square active area of 1.8×10^{-4} cm^2. Both tables list the operating points, i.e., the incident CO_2 laser power, the bias voltage, the dark current, and the local oscillator induced current at which the NEP and effective heterodyne quantum efficiencies were measured.

The effective heterodyne quantum efficiencies have been measured to be fairly flat in the 100 to 2000 MHz frequency range. Figure 7 presents data showing the measured effective heterodyne quantum efficiency as a function of frequency for element 2 of the four element array whose properties are listed in Table 2. The device exhibited an effective heterodyne quantum efficiency of 19%

at 2.0 GHz when reverse biased to 0.450 volts and with 0.641 milliwatts of CO_2 laser power focused onto the photodiode active area.

All of the effective heterodyne quantum efficiencies listed in Tables 2 and 3 were measured at 2.0 GHz. The incident CO_2 laser powers required to provide the listed effective heterodyne quantum efficiencies ranged from approximately 0.295 to 1.090 milliwatts. These power levels resulted in photoinduced currents of 1.4 to 2.5 mA. It is entirely possible to increase the effective heterodyne quantum efficiency by utilizing larger levels of incident CO_2 laser power. However, saturation effects and thermal damage may result from the use of increased laser power levels.

CONCLUSION

The measurements presented for the n^+-p $Hg_{0.8}Cd_{0.2}Te$ photodiode show that it is possible to use it as a moderate bandwidth, 10.6μm CO_2 laser heterodyne detector. This diode may be operated at either 77 K or 145 K with a fairly good sensitivity. By proper adjustment of the (Hg,Cd)Te bandgap and doping levels on either side of the n-p junction, it should be possible to use the n^+-p device structure cooled to the temperature range of 185 to 205 K for 8-14 micrometer infrared heterodyne applications.

Single element and four element n^+-n^--p (Hg,Cd)Te photodiode arrays have been developed for 10.6μm wide bandwidth CO_2 laser heterodyne applications. Effective heterodyne quantum efficiencies of approximately 13 to 30% at 2000 MHz have been exhibited. The photodiode's frequency response and heterodyne sensitivity may be improved by the proper choice of junction geometry, by microwave matching of the photodiode's output to the wide bandwidth preamplifier, by the application of an anti-reflection coating to the photoactive area, and by optimizing the junction depth and the depletion region width.

Current research and development is aimed at developing arrays (12 elements) and increasing the bandwidth and heterodyne sensitivity of the n^+-n^--p$(Hg_{0.8}Cd_{0.2})$Te photodiode.

REFERENCES

1. J.F. Shanley and L.C. Perry, Proceedings of the IEEE International Electron Devices Meeting, Washington, D.C. (1978), pp. 424-429.

2. D.L. Spears, Proceedings of the IRIS Detector Specialty Group Meeting, U.S. Air Force Academy, CO (1977).

3. A.K. Sood and T.J. Tredwell, Proceedings of the IEEE International Electron Devices Meeting, Washington, D.C. (1978), pp 434-436.

4. A.K. Sood and S.P. Tobin, IEEE Electron Device Letters, EDL-1, No. 1, January 1980.

5. K.J. Riley, J.M. Murosznyk, P.R. Bratt and A.H. Lockwood, Proceedings of the IRIS Detector Specialty Group Meeting, Minneapolis, MN (1979), pp 199-207.

6. J.F. Shanley and C.T. Flanagan, Lasers '79 Conference, Orlando, Florida, 17-21 December 1979.

7. B.J. Peyton, et. al, IEEE J. Quant. Electron., Vol. QE-8, 2, February 1972.

8. G. Lucovsky, M.E. Lasser and R.H. Emmons, Proc. IEEE, 51, 166 (1963).

9. S.M. Sze, Physics of Semiconductor Devices, pp. 663-667, John Wiley and Sons, New York (1969).

10. D.E. Sawyer and R.H. Rediker, Proc. IRE, 46, 1122, June, 1958.

11. R.P. Riesz, Rev Sci Instr. 33, 994, September 1962.

Table 1.

Characteristics Of A Three Element $n^+ - p$ Photodiode Array At Temperatures Of 77 K And 145 K

ELEMENT	TEMPERATURE (K)	CUTOFF WAVELENGTH (μm)	FORWARD RESISTANCE (ohms)	ZERO BIAS RESISTANCE (ohms)	BREAKDOWN VOLTAGE (volts)	DC QUANTUM EFFICIENCY (%)	BIAS VOLTAGE (mV)	CAPACITANCE (pF)	DARK CURRENT (mA)	INCIDENT CO_2 LASER POWER (mwatts)	HETERODYNE SIGNAL FREQUENCY RESPONSE (MHz)	NOISE EQUIV POWER (NEP) (W/Hz)	EFFECTIVE HETERODYNE QUANTUM EFFICIENCY (%)
1	77	13.83	20.5	100	0.240	78	160	20.4	0.55	0.268	625	3.2×10^{-20}	58
	145	11.10	19.38	30	0.046	78	240	27.7	1.85	0.400	675	1.0×10^{-19}	19
2	77	13.66	21.0	102	0.230	73	90	23.9	0.35	0.322	725	8.4×10^{-21}	22
	145	11.07	20.63	40	0.060	74	200	19.1	1.5	0.201	600	1.2×10^{-19}	16
3	77	14.11	19.0	75	0.200	76	55	26.5	0.15	0.263	500	8.8×10^{-21}	21
	145	11.40	18.5	34	0.032	75	250	17.7	1.65	0.180	475	1.3×10^{-19}	14

Table 2.

Summary Of Single Element $n^+ - n - p$ $Hg_{0.8}Cd_{0.2}Te$ Photodiode Low Frequency And Heterodyne Characteristics

MIXER	BREAKDOWN VOLTAGE (VOLTS)	AREA (cm^2)	λ_{peak} (μm)	λ_{co} (μm)	R_o (ohms)	$R_{forward}$ (ohms)	BIAS VOLTAGE (VOLTS)	R_o (ohms)	C (pF)	L (nH)	η_{DC}	BANDWIDTH	I_{LO} mA	P_{LO} (mW)	NEP (J/Hz)	η_{EH}
1	1.72	1.8×10^{-4}	10.0	10.88	410	16	0.75	2000	1.75	0.75	56%	$\geq$ 2.0 GHz	1.4	0.360	1.1×10^{-19}	17%
2	0.86	1.8×10^{-4}	10.5	12.5	180	13.3	0.3	1000	2.8	0.77	62%	$\geq$ 2.0 GHz	1.8	0.295	6.45×10^{-20}	29%
3	0.70	1.8×10^{-4}	10.5	16.06	375	17	0.35	740	1.58	0.67	56%	$\geq$ 2.0 GHz	2.2	0.330	1.24×10^{-19}	15%
4	0.63	1.8×10^{-4}	11.0	11.66	367	20	0.32	600	1.48	0.80	65%	$\geq$ 2.0 GHz	1.8	0.310	1.44×10^{-19}	13%
5	1.49	1.8×10^{-4}	10.5	11.41	778	16	0.34	3330	4.9	3.1	52%	$\geq$ 2.0 GHz	2.0	0.330	6.23×10^{-20}	30%
6	1.76	1.8×10^{-4}	10.5	11.5	775	16	0.33	4680	5.06	3.3	34%	$\geq$ 2.0 GHz	2.5	1.09	7.79×10^{-20}	24%

Table 3.

Summary Of The Heterodyne Characteristics Of A Four Element $n^+ - n^- - p$ $Hg_{0.8}Cd_{0.2}Te$ Photodiode Array

ELEMENT	λ_{co}	λ_p(μm)	η_{DC}	RF (ohms)	R_o (ohms)	BREAKDOWN VOLTAGE (VOLTS)	I_{LO} (mA)	P_{LO} (mA)	V_{BI} (VOLTS)	NEP (W/Hz)	η_{EH}	DARK CURRENT (mA)
1	11.5	10.5	0.375	28.5	270	1.7	2.35	0.716	0.35	6.93×10^{-20}	27%	100
2	11.18	10.5	0.50	33.3	250	1.8	1.98	0.641	0.450	9.84×10^{-20}	19%	100
3	11.5	10.5	0.385	29	270	0.80	2.0	0.633	0.180	1.34×10^{-19}	14%	200
4	11.5	10.5	0.365	25	500	2.1	1.95	0.656	0.530	1.31×10^{-19}	14.3%	50

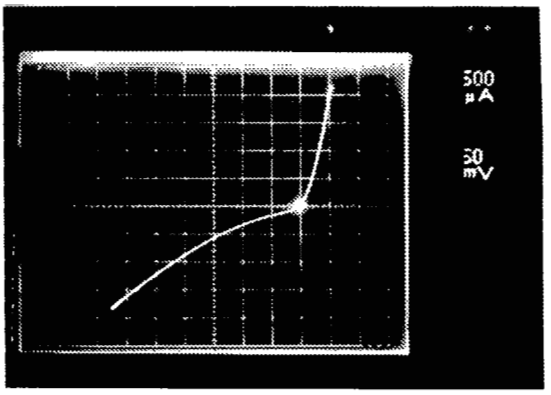

T = 77
λ_{co} = 13.83μm
V_B = 0.240 volts
$R_{FORWARD}$ = 20.5
R_o = 100 ohms
A = 1.8×10^{-4} cm^2

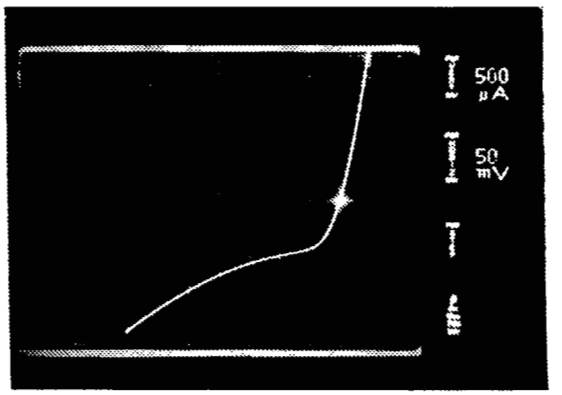

T = 145
λ_{co} = 11.10μm
V_B = 0.046 volts
$R_{FORWARD}$ = 19.38 ohms
R_o = 30 ohms
A = 1.8×10^{-4} cm^2

Figure 1.- I-V characteristics of element 1 measured at 77 K and 145 K.

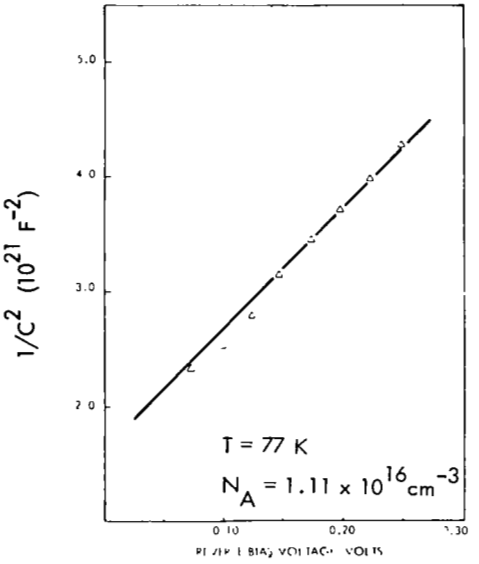

Figure 2.- $1/C^2$ versus reverse bias voltage for element 1.

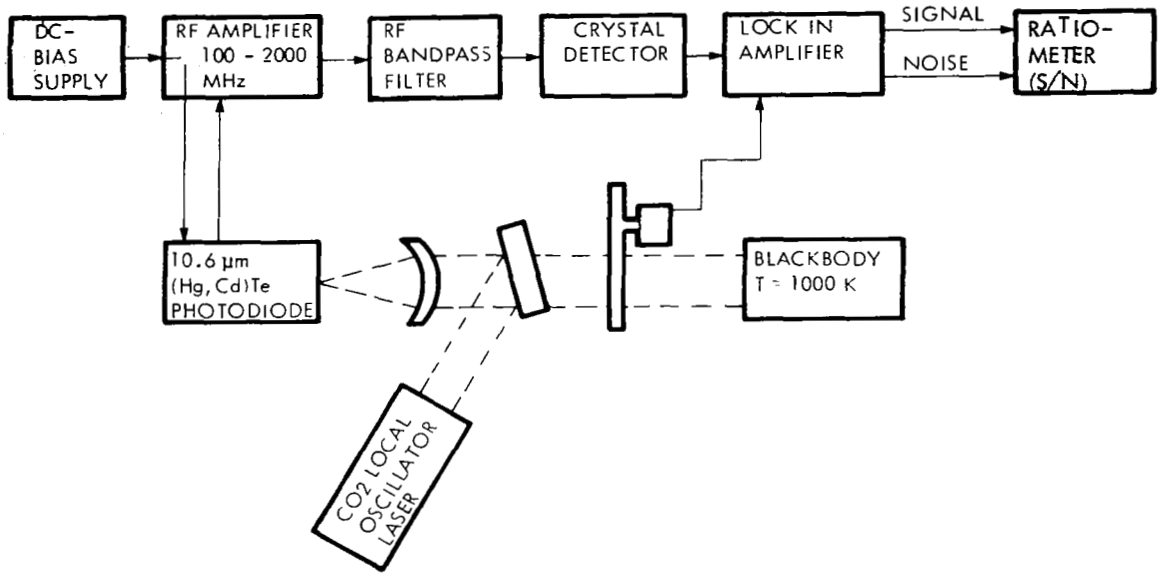

Figure 3.- Heterodyne radiometer.

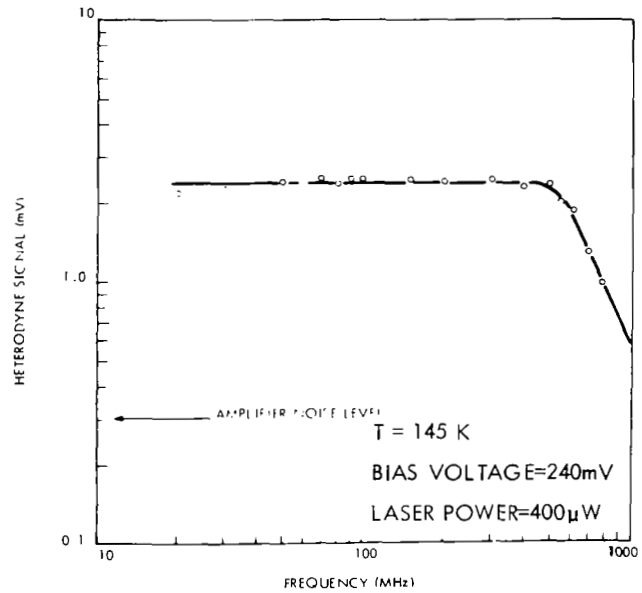

Figure 4.- Heterodyne signal frequency response of element 1 measured at 145 K.

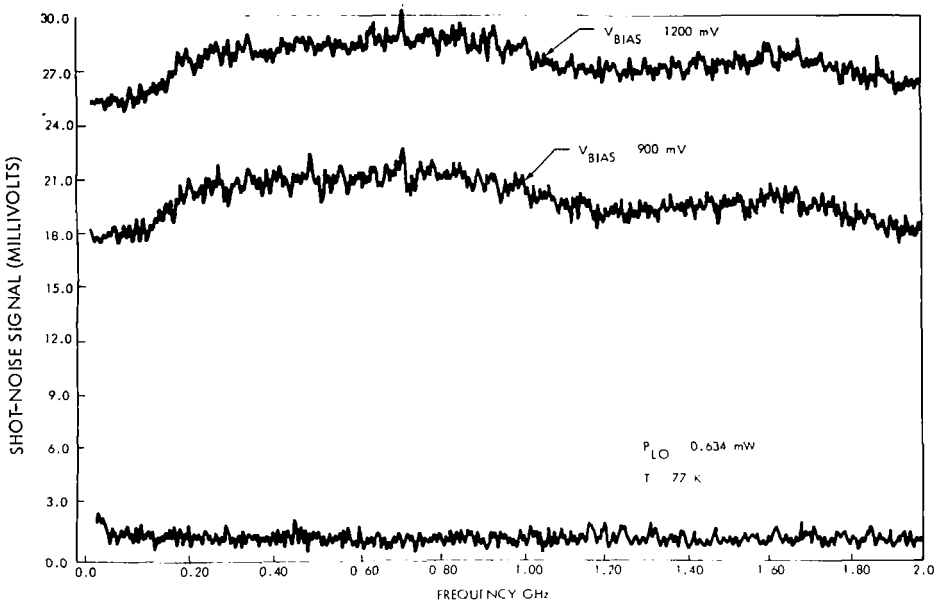

Figure 5.- Shot-noise signal response versus frequency for element 2 of a four element array.

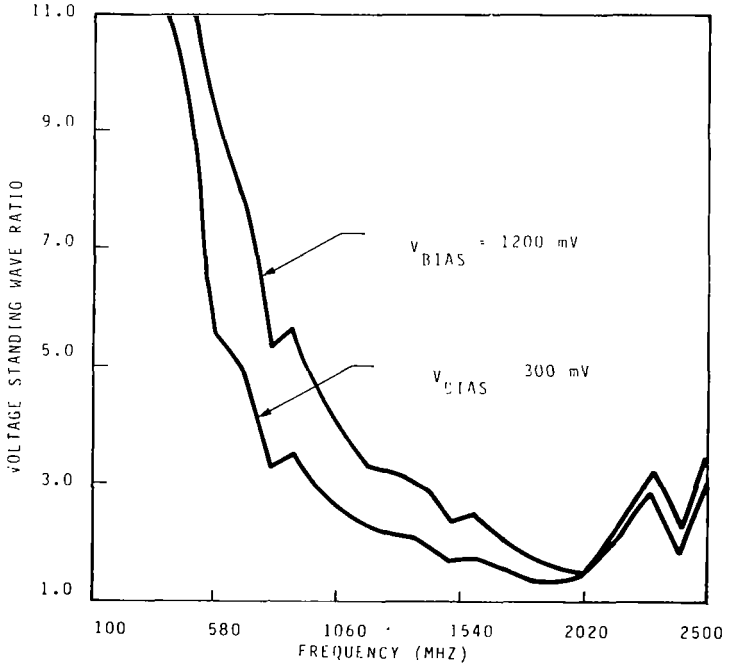

Figure 6.- Voltage standing wave ratio versus frequency for element 2 of a four element array.

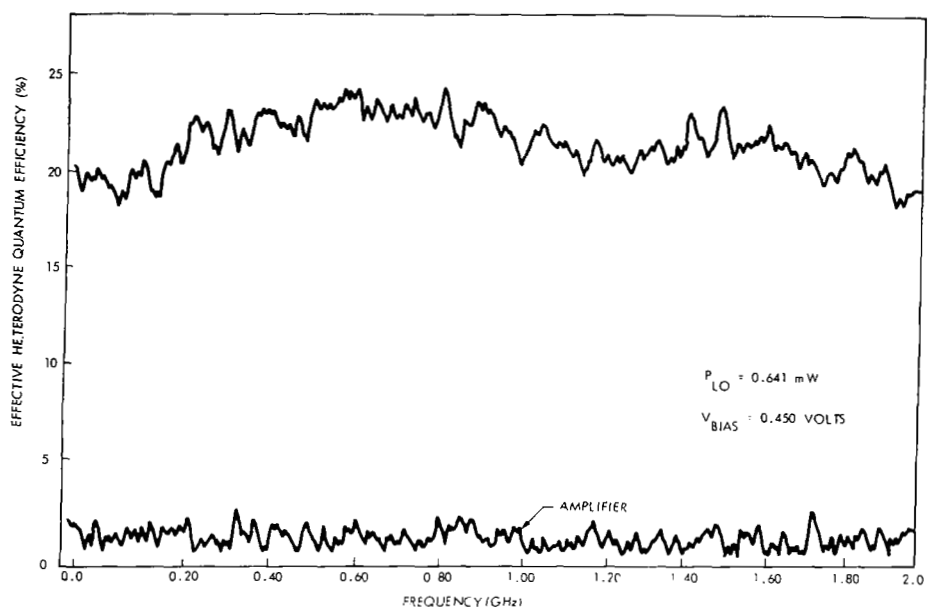

Figure 7.- Effective heterodyne quantum efficiency versus frequency for element 2 of a four element photodiode array.